Carbonates and Evaporites (2020) 35:79
https://doi.org/10.1007/s13146-020-00615-3

ORIGINAL ARTICLE

# The local variation of the overlying soils geotechnical properties in the karst susceptibility assessment

**Elena Drobinina[1] · Tatyana Kovaleva[2] · Anna Koriakina[1]**

Accepted: 28 June 2020 / Published online: 6 July 2020


**Abstract**
The technique of karst susceptibility assessment in the territory of Ust-Kishert village is presented. The environmental conditions of predominantly gypsum and carbonate–gypsum karst area are analyzed. The zonation map of karst cavities and crushed zones density is created. The distribution of the overlying soil geotechnical property values within the classes of different subterranean karst form density is carried out and presented in the form of histograms and distribution curves. The computer simulation of the soil stress condition is used to demonstrate that karst cavity affects the mechanical properties of the overlying soils and alters the initial stress in the soils. In our research, the anomalous values of the overlying soil geotechnical properties are applied as the indicators of the karst cavities and crushed zones location. The anomalous value intervals are determined by one-dimensional statistical analysis. The analysis of the overlying soil geotechnical properties is resulted in the integral model of karst susceptibility in the research area.

**Keywords** Geotechnical properties · Susceptibility · Sinkhole · Subsidence · Cavity · Crushed zone · Overlying soil · Sulfate karst · Ust-kisert village

## Introduction

According to Gutiérrez et al. (2014), there are two types of predictive model of sinkhole formation: hazard models and susceptibility models. The hazard models represent quantitative probability estimation for a given zone and time interval of being affected by a sinkhole event. The relative probability of a sinkhole occurring in any specific place is provided by susceptibility models.

Varnes (1984) holds a similar opinion relating to hazard. According to him, natural hazard means the probability of occurrence within a specified period of time and within a given area of a potentially damaging phenomenon.

In the research, susceptibility models are represented. The study area is categorized by degree of danger of a sinkhole formation based on changes of the overlying soil geotechnical properties, such as soil density, friction angle and cohesion. In terms of this research, the changes of the soil properties are believed to be indicators karst cavities and crushed zones existence in bedrock.

✉ Elena Drobinina
alenadrobinina@yandex.ru

[1] Laboratory of Prognostic Modeling in Geosystems, Perm State University (PSU), Perm, Russia

[2] Faculty of Geology, Perm State University (PSU), Perm, Russia

## Theoretical statements and geological model of research

Karst landforms develop especially in carbonate rocks, but also in gypsum (Gutiérrez and Cooper 2013). The rate of limestone dissolution is negligible at a human time scale. Sinkholes are associated with old pre-existing cavities formed in the geological past that have become unstable now due to different changes in the karst environment. Conversely, the gypsum high-rate dissolution may lead to create and expand cavities and reduce the rock mass strength bringing to sinkhole development in the short term (Parise et al. 2015). In areas where carbonates are interbedded with gypsum, the potential for the gypsum dissolution is large (Zhou and Beck 2011).

Surface karst forms result from both subsurface dissolution and downward gravitational movement of the undermining overlaying material at covered karst called *merokarst* or mantled karst (Milanović 2018). They

have spontaneous occurrence resulting in significantly complication of the territories economic development. Moreover, collapse sinkholes develop very fast and, therefore, it impossible to take the necessary measures for averting the buildings damage especially if the protective constructive measures were not accepted.

In this work, we consider *karst massif* as a certain volume of geological space occupied by the soluble rocks and the overlying soils that are affected by the karst process. The dissolution of soluble rocks, erosion, accumulation and gravitational collapse cause the variability of the karst massif properties in various points (Kataev 2004).

The purpose of this study is to identify the areas of local changes of overlying soil geotechnical properties relative to the background one. It is our belief that these areas are the most probable location of karst cavities and crushed zones in bedrock.

The overlying soil mass functions as a typical *dissipative* system in nonequilibrium conditions associated with the cavities formation in the bedrocks. This system is able to evolve and create ordered structures (in this case, deformational ones) due to the process of self-organization of the geological environment (Anikeev 2017). Thus, it is believed that the karst cavity formation in the bedrock leads to a change in the properties of overlying soils up to their deformation and sinkhole formation. That is associated with the stress removal that is capable to trigger the downward gravitational movement of soils into the karst cavity.

The model of limit state of overlying soils above a cavity was developed by Postoev (2013). The prerequisite for the sinkhole and subsidence formation depending on the geological structure and soil properties are considered. According to the model, the karst cavity formation at the contact of bedrock and overlaying soils triggers stress removal and soil deformation above the cavity in karst massif initially stable under the Mohr–Coulomb law.

Mohr–Coulomb failure criterion (Churinova 1968) states that the parameters describing the mechanical properties of cohesionless (1) and cohesive (2) soils are in the following dependence on the principal stresses $\sigma_1$ and $\sigma_3$:

$$\sin\varphi = \frac{\sigma_1 - \sigma_3}{\sigma_1 + \sigma_3}, \tag{1}$$

$$\sin\varphi = \frac{\sigma_1 - \sigma_3}{\sigma_1 + \sigma_3} - \frac{2c\cos\varphi}{\sigma_1 + \sigma_3}, \tag{2}$$

where $\varphi$ is the friction angle, and $c$ is the cohesion.

The computer simulation of the soil stress condition demonstrates that karst cavity affects the mechanical properties of the overlying soils and alters the initial stress in the soils (Figs. 1 and 2). Figure 1 demonstrates typical section of borehole used in the computer simulation that shown on Fig. 2.

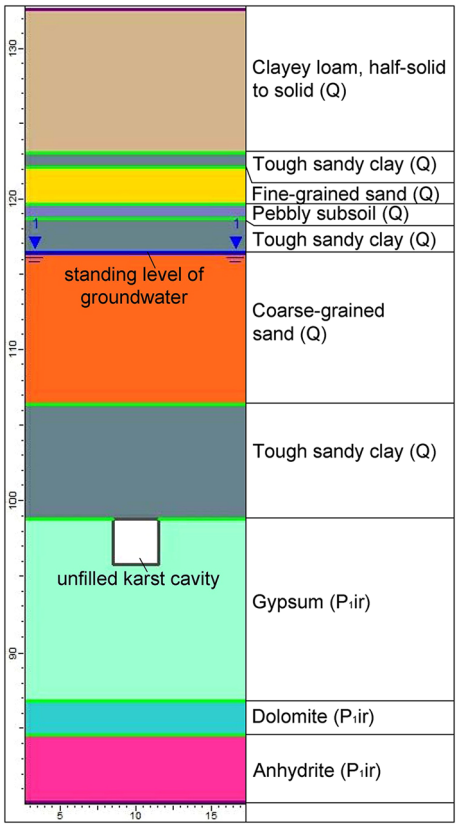


**Fig. 1** Typical section of borehole

## Short characteristics of the research area

The research area is situated in the southeast of the Perm region, Russia (Fig. 3) within Ust-Kishert village. It is located in predominantly gypsum and carbonate–gypsum karst area of the Kishert district (Gorbunova et al 1992).

### Tectonics

The research area is situated at eastern edge of the East European Platform, more precisely within the northern part of the Ufimskoe plateau and the Pre-Urals foredeep within the Sylvinskaya depression. The broad distribution of the tectonic faults, which is clearly traced in aerial and satellite imagery, indicates the high tectonic activity of the research area. According to Milanović (2018), sinkholes frequently orientate in the longest fault or fault zones direction.

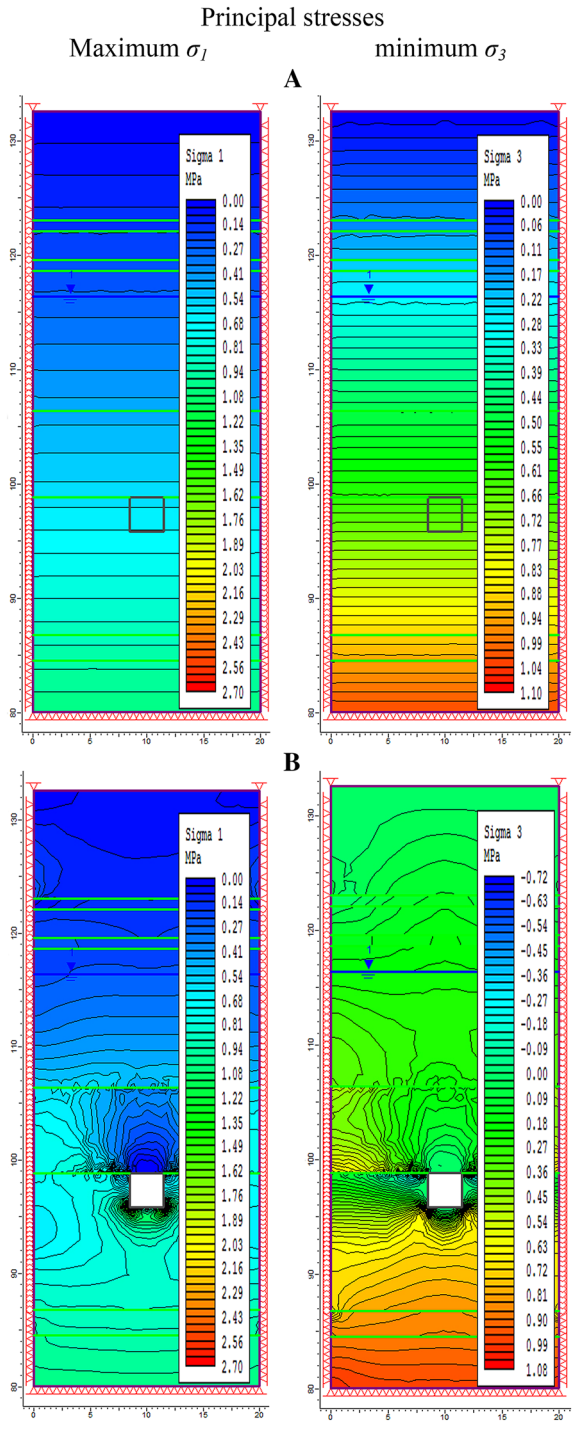


**Fig. 2** Computer model of the soil stress. **a** Without karst cavity, **b** with karst cavity in the roof of bedrock

## Geology

At the baseline, the geologic profile of the research area is represented by limestone, dolomite, gypsum and anhydrite interbedded each other and with clay (Artinskian and Kungurian stages of Cisuralian series Permian system). Carbonate layers often wedge out of the geologic profile, replaced by sulphates. In these places, large karst cavities are formed and filled with crushed stone, blocks and clay material. The sulfate stratum is unevenly fractured. In the upper part of the stratum and near large karst cavities, sulfate rocks are highly fractured and weathered. Cracks of various directions are filled with white gypsum, dolomite, rare with clay material or fibrous selenite.

Non-karst deposits with karst blocks named karst-collapsed formations (Neogene and Quaternary systems) are overlaid with the bedrock in some places. There are several types of karst-collapsed formations: (1) calcareous clays, loam and sandy loam with bedrock rubble and debris, (2) gravel and pebble subsoils with bedrock rubble and debris, (3) gravel and pebble bedrock with clayey or loamy fill and rare siliceous gravel and pebbles and (4) blocks of bedrock.

Fluvial and alluvial formations (Quaternary system) are overlaid with the bedrock everywhere. Quaternary deposits within Ust-Kishert village are up to 65.0 m in thickness and comprise loams, clays, sandy loams, sands and gravel-pebbly soils. Deluvial and eluvial deposits are rare and presented by soil of sandstone or limestone rubbles and debris with clayey fill (30%). The soil is exposed in the form of separate lenses under the alluvial deposits at the depth of 2.5–13.5 m and has the thickness of 2.4–15.0 m.[1]

## Hydrogeology

There are groundwater and karst aquifers in research area. Groundwater is developed in alluvial deposits of Sylva river valley, such as loam, sandy loam, gravel and pebble soils. The depth of groundwater level varies from 15 to 1 m in the direction to Sylva river. Groundwater is recharged by atmospheric water infiltration chiefly but in areas where the impervious layer is missing groundwater is recharged from karst aquifer. Groundwater is predominantly fresh (mineralization is up to 1 g/dm$^3$).

Karst aquifer is developed in carbonate and sulfate rocks of Kungurian stage. In karst aquifer, the water circulation is available to large cracks and cavities on the contacts between sulfate rocks, limestones, alluvial sediments, and brecciated bedrock. The circulation is accompanied by the bedrock dissolution with new subterranean karst forms formation. The depth of circulation is determined by the erosion base level.

The depth of karst aquifer level varies from 15 to 40 m. The predominant mineralization is about 2 g/dm$^3$.

The recharge of karst aquifer takes place in Ufimskoe Plateau, where atmospheric precipitation is absorbed and

[1] Kataev V.N. Report on the research work "Monitoring of the karst territories of the Perm Region", Perm, 2010.

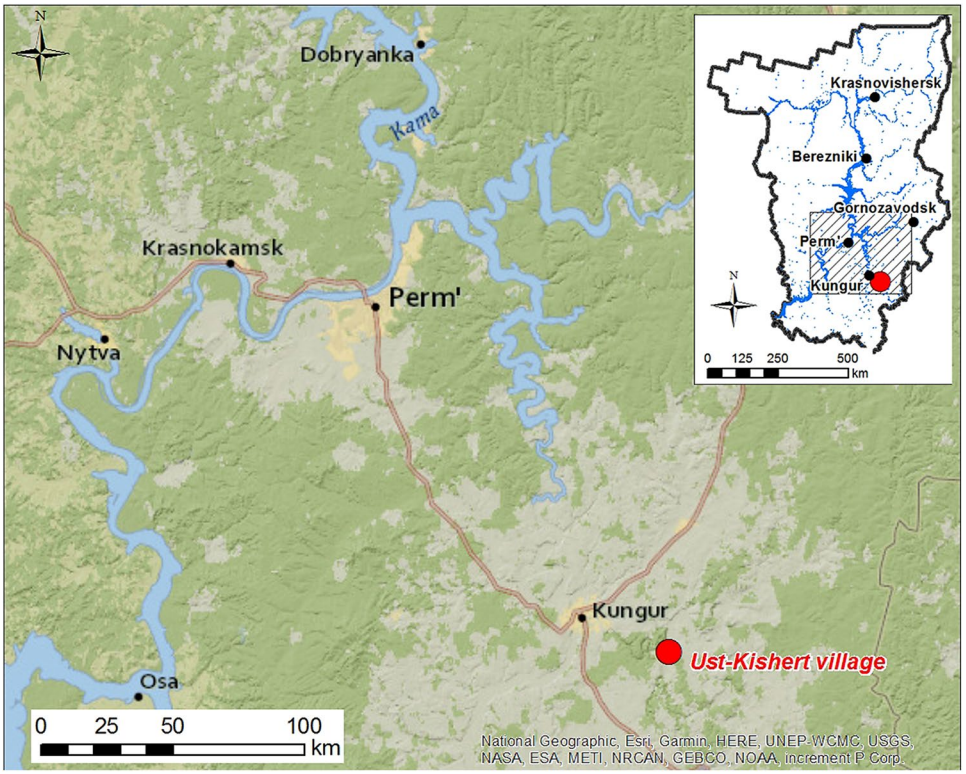


**Fig. 3** The location of the research area in Perm region territory

reached soluble bedrocks. Then, water direct towards the places of discharge along the dip of the layers. In addition, karst aquifer could be recharged by surface water from lakes, rivers. Sinkholes usually develop as a drainage point into a subsurface conduit system through which water with suspended sediments, including contaminants is carried into the aquifer (Zhou and Beck 2011).

## Karst

The most representative morphological surface and subterranean forms associated specifically with research area are sinkholes and karst cavities. There are peculiar type of forms named crushed zones that are represented weakened sections of the karst massif, characterized by a high degree of fragmentation and fracturing. Consequently, these elements have a high hydrogeological and hydrochemical activity and include the zones with high density of oriented fractures, crushed zones, faults, etc. (Kataev 1994).

Sinkholes are frequently called dolines in scientific literature (Waltham and Lu 2007; Ford and Williams 2007; Milanović 2018), but in this research, we use sinkholes for any enclosed depressions karst-related.

Sinkholes that are abundant in the research area are formed by collapse of the karst cavities roofs with overlying sediments and named *dropout sinkholes*. In case if only the soluble rocks move downward, the cavity *collapse sinkholes* will form (Waltham et al. 2005). According to Nisio et al. (2007), collapse sinkholes are also called *cave-collapse sinkholes* and dropout ones are also called *cover-collapse sinkholes* due to the main genetic processes.

Moreover, there are two types of sinkholes in the overburden: *cover-collapse* and *cover-subsidence* which differ by the formation rate depending to the type of void contact (soil/rock) with overlying sediments (Zhou and Beck 2011; Gutiérrez et al. 2014). In the research area, cover-collapse sinkholes are widespread.

Within the gypsum karst, sinkholes are often a result of collapsing caves, formed within the gypsum and anhydrite bedrock (Kaufmann 2014), which in an aqueous solution dissolve rapidly. The initial dissolution rates of anhydrite are lower by a factor of 20 compared with gypsum (Dreybrodt 2006).

Sinkholes were identified by digitizing topographic maps and data of archival karstological research carried out in the area by Perm State University. In addition, the sinkholes are mapped on sensing data, such as satellite images. The remote sensing data are often used to detect the karst forms distribution. For example, Brinkmann et al. (2007) used for the same purpose aerial photographs from 1926 and 1995 that covered the urbanized Pinellas County, Florida, USA.

According to observations survey by scientists of Perm State University, 120 pcs. surface karst forms, 60 pcs. karst cavities and 24 pcs. crushed zones are fixed within Ust-Kishert village.

**Fig. 4** The typical sinkhole in the research area (Photo provided by E. Drobinina)

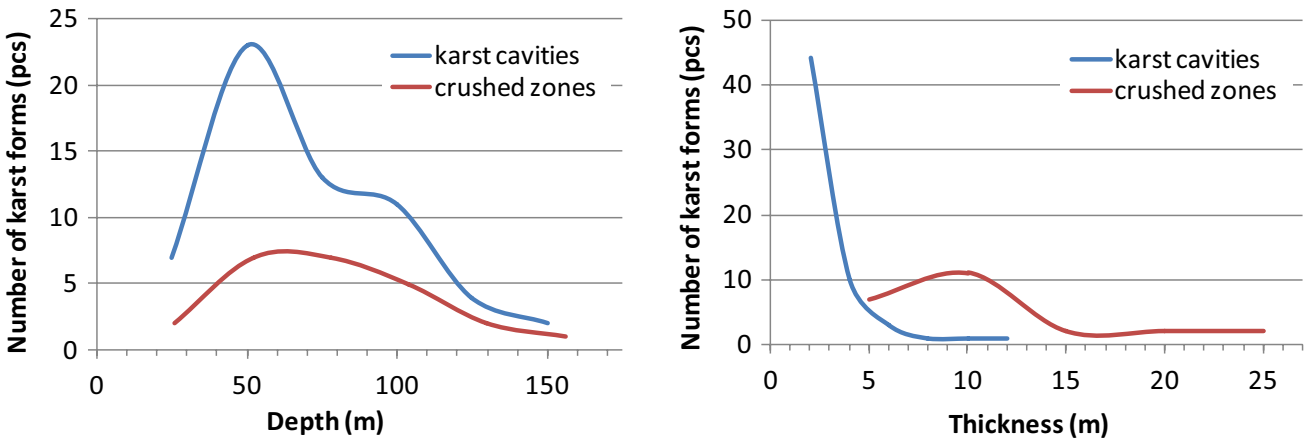


**Fig. 5** A graphs of the karst cavities and crushed zones distribution

All surface karst forms are represented by cover-collapse sinkholes. In the research area, sinkholes form by sudden downward gravitational movement of unconsolidated alluvial sediments into karst cavities, occurred in gypsum, predominantly on the gypsum–limestone contacts. The typical sinkhole is shown in the Fig. 4.

Sinkholes vary in shape and size. Plate and long depression are prevailed, that is about 40% each, the rest of sinkholes (20%) is characterized as the funnel shape. Sinkholes' average diameters are very diverse, from 2 m upward of 100 m. The largest sinkhole diameters are typified the karst lakes and Molebnoe lake, for example.

The karst cavities are encountered in boreholes in the depth of 20–80 m predominantly. The total cavity thickness in the wells varies from 0.5 to 5 m. The exception is the northern part of the area where three cavities with a total thickness of 18 m were encountered in the borehole (Fig. 5). There are no karst caves with the orifice to the surface in the research area.

There are peculiar subterranean forms named crushed zones. This is not a typical karst form which was initially formed by dissolution of bedrock. Crushed zones are formed by weathering; however, high fracturing is favorable to bedrock dissolution and decrease in the stability of the

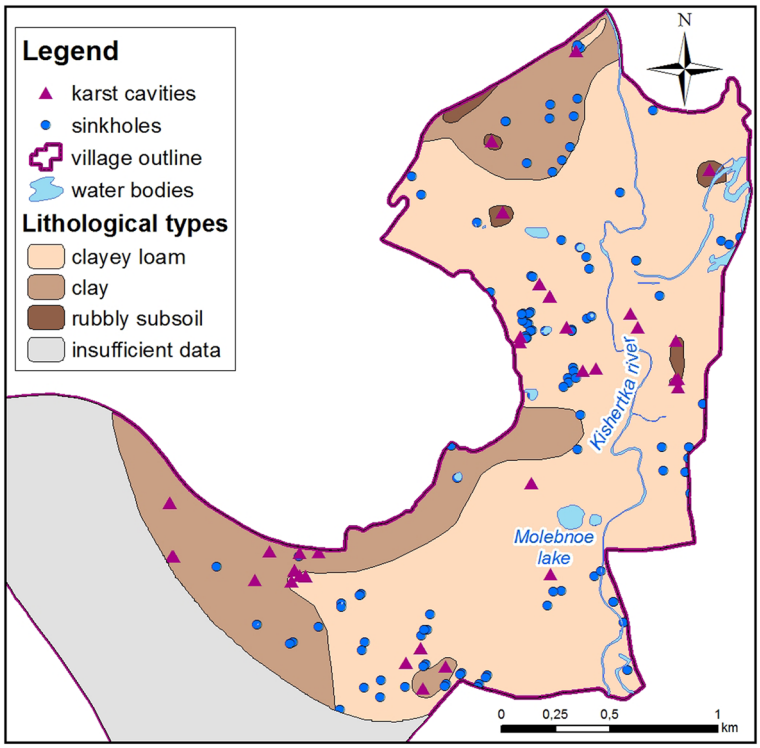


**Fig. 6** The distribution map of lithological types of Quaternary sediments and karst forms (map projection: EPSG:3395 WGS84/ World Mercator; Shilova and Kovaleva 2015)

massif. Crushed zones occur at the depths of 25–82 m. Their total thickness is 5–15 m and in rare cases, the vertical size of the crushed zones does not exceed 10 m (Fig. 5).

Karstological survey, such as the study of surface and subterranean karst forms, the geology and hydrogeology, has been carried out in Ust-Kishert village regularly over the past 60 years by the Department of Dynamic Geology and Hydrogeology of Perm State University. The data of geotechnical investigation for civil engineering in the research area were used as input data for analysis. These data are reliable as a result of strict control of these geotechnical investigation by regulatory framework.

According to long-term observations survey of the Quaternary overlying soils, the authors' maps of their lithological composition and thickness (Figs. 6 and 7) are made. The western part of Ust-Kishert village is not sufficiently explored; thus, there is no conditioned data for this part of the study area (Shilova and Kovaleva 2015).

Quaternary sediments represented by loam (2.89 $km^2$) occupy the most part of the study area (from the south–west to the north of the village). The central and northern parts are represented by clays (1.31 $km^2$). The smallest area is occupied by sediments represented by gravel (0.07 $km^2$) and located in the southeastern part of the territory. To the west, there are bedrock exposures (0.27 $km^2$) (Shilova and Kovaleva 2015).

The maximum thickness of Quaternary deposits (more than 50 m) occurs in the northeastern part of the study area. Small areas with a cover thickness of more than 40 m are encountered in the central and southwestern parts. Ust-Kishert village occupies the areas with a thickness of Quaternary deposits of 10–25 m (3.7 $km^2$) (Shilova and Kovaleva 2015).

Most of the karst cavities (22 pcs, 39.3%) were located in the areas with Quaternary deposits of 15–20 m in thickness. The maximum number of karst sinkholes (30 pcs, 30%) is confined to the areas with a similar thickness of the Quaternary sediments (15–20 m, Fig. 7) (Shilova and Kovaleva 2015).

The zonation map of karst cavities and crushed zones density was created and presented by the method of natural breaks in three classes depending on the one's number per unit area: low density—0–6.5 pcs/$km^2$, medium one—6.5–18.5 pcs/$km^2$, high one—18.5–33.5 pcs/$km^2$ (Fig. 8).

The distribution of the overlying soil geotechnical property values within the classes of different density carried out and presented in the form of histograms and distribution curves (Fig. 9). The influence of karst cavities and crushed zones on the overlying soil geotechnical properties is noted. There is a decrease in soil density with an increase in the density of karst cavities and crushed zones from 1.82 g/$cm^3$ for medium- and low-density areas to 1.77 g/$cm^3$ for high-density areas. Values of cohesion with an increase in the density of karst cavities and crushed zones are reduced from 25 to 26 kPa for low- and medium-density, respectively, to 24 kPa for high-density areas. Conversely, values of friction angle increase from 18 to 23° with an increase the density of karst cavities and crushed zones.

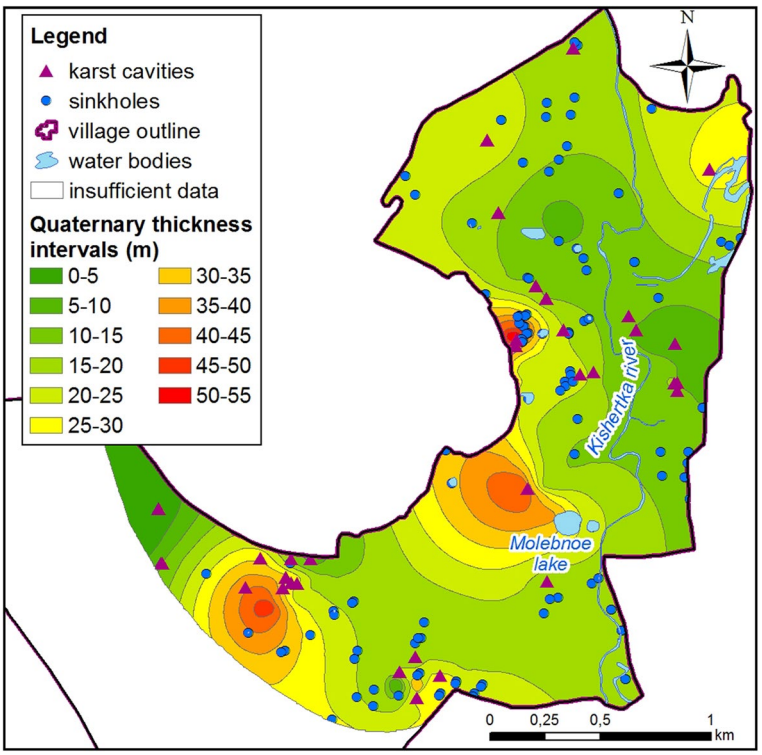


**Fig. 7** The map of Quaternary sediments thickness and karst forms (map projection: EPSG:3395 WGS84/World Mercator; Shilova and Kovaleva 2015)

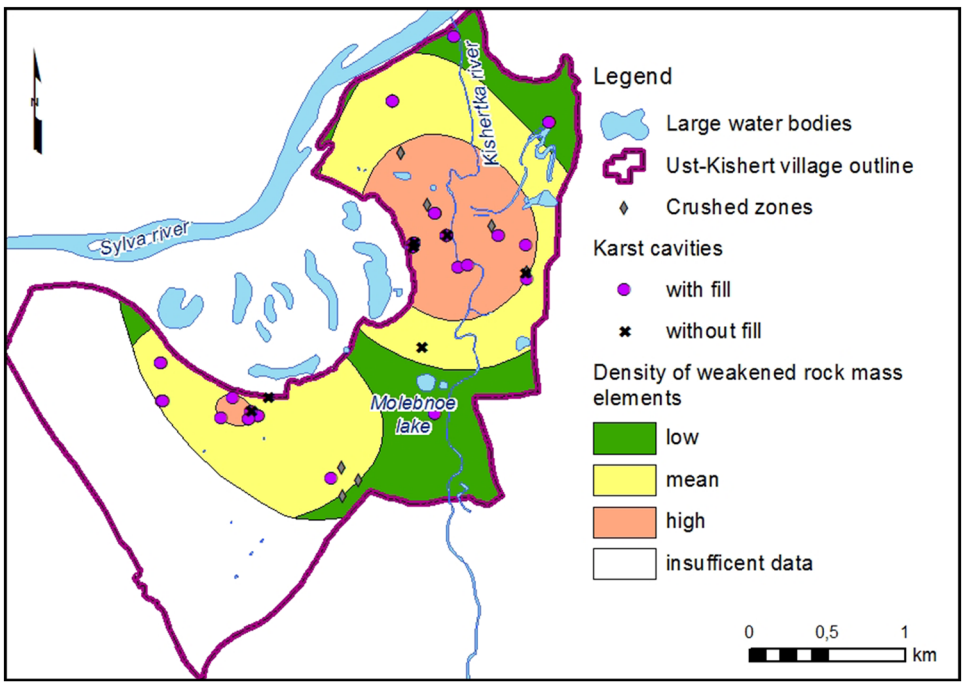


**Fig. 8** The zonation map of karst cavities and crushed zones density (map projection: EPSG:28,410 Pulkovo 1942/ Gauss-Kruger zone 10)

## Research methodology

One of the modern tasks of engineering karst is the prediction of the possible karst deformation location and size. A precise collapse probability assessment is reached by the analysis of the stability conditions of caves, like it represented by Parise (2015), for example. However, if karst caves do not have access to the surface or karst cavities are small in size, indirect methods of investigating the subterranean karst ought to be applied. Thus, the use of various indicators is applied.

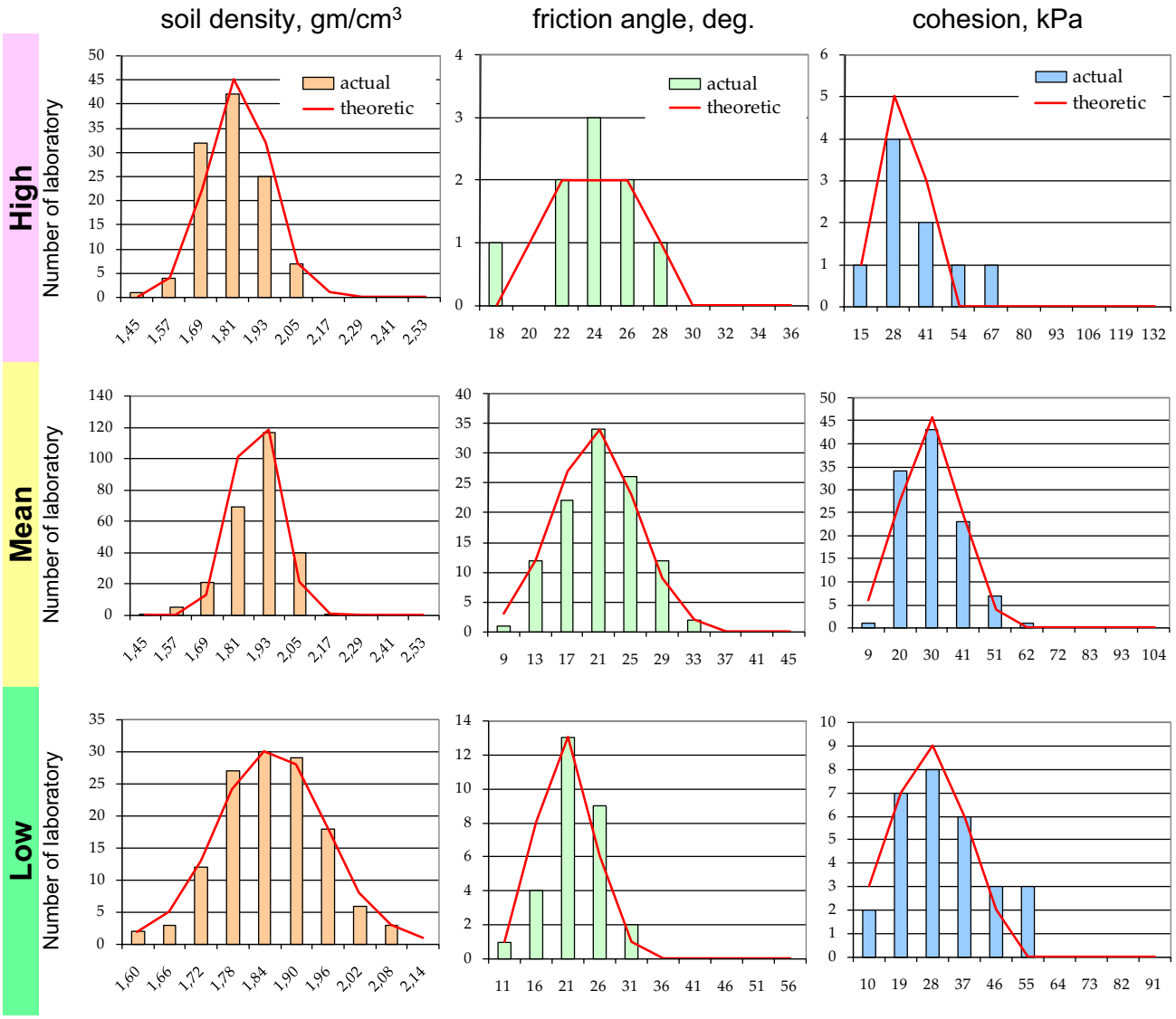


**Fig. 9** The distribution of the overlying soil geotechnical properties within the allocated classes of different subterranean karst form density

Geophysical methods are often used for remote measurements of subterranean karst. For example, ground penetrating radar (GPR) as the most resolute method, seismic reflection (SR) and electrical resistivity tomography (ERT) were applied to locate the main karst cavities and caves (Margiotta et al. 2016).

In our research, the anomalous values of the overlying soil geotechnical properties are applied as the indicators of the karst cavities and crushed zones location. The anomalous value intervals are determined by the one-dimensional statistical analysis.

Only the Quaternary clay and loam from plastic to solid consistency were analyzed in this research because of the sufficient number of laboratory mechanical properties measurements. The fluid-plastic and fluid soils were not involved due to the sharp variability of their mechanical properties after water saturation.

According to Terzaghi (1996), the increase of water content in soil is accompanied by the three effects: (1) redistribution of water molecules and ions in adsorbed layers, (2) reorientation of clay particles and (3) breakdown of sedimentation and consolidation structure of clays. For example, for clayey soils of the high-plastic consistency, the friction angle does not exceed 5–10°. Low-plastic and solid clays are characterized by the friction angles of 14–35°. The water saturation of sandy soils decreases the friction angle by 1–2°. The effect of water content on the shear resistance becomes particularly noticeable in the soils containing clay and silt fraction (Paniukov 1962).

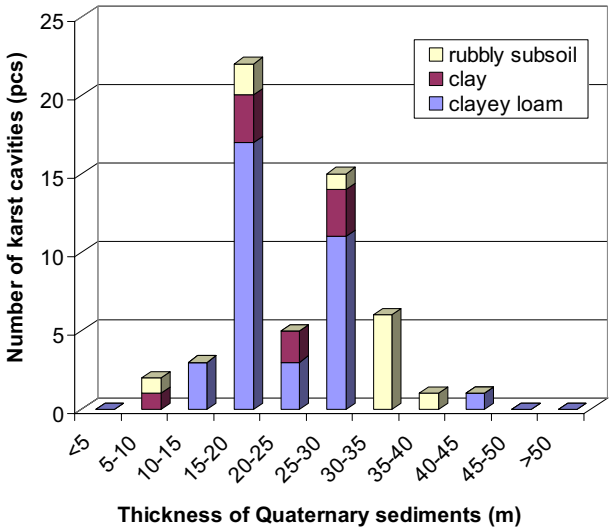


**Fig. 10** Distribution of the karst cavities subject to lithology and Quaternary sediments thickness (Shilova and Kovaleva 2015)

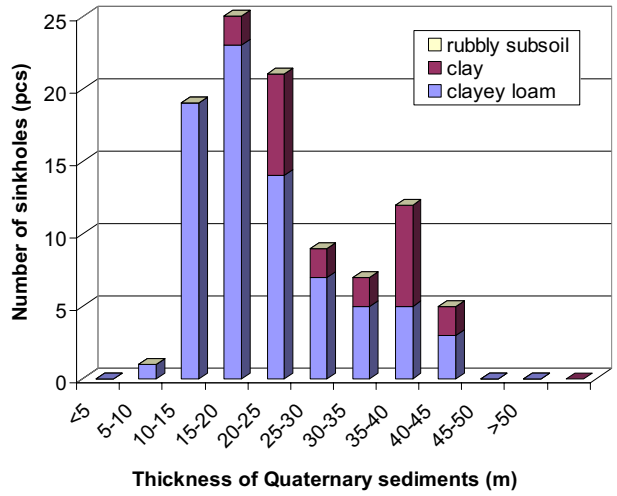


**Fig. 11** Distribution of the sinkholes subject to lithology and Quaternary sediments thickness (Shilova and Kovaleva 2015)

The properties of clayey soils have been investigated by the authors earlier. It was concluded that the most karst-susceptible areas are those where loams with the thickness of 10–25 m are predominant. The largest number of karst cavities is found in the areas where loams have a thickness of 15–20 m (17 pcs, 48.6%) and 25–30 m (11 pcs, 31.4%) (Fig. 10). The areas composed of loams have the highest karst sinkholes occurrence (56 pcs, 72.8%) (Fig. 11).

All the values of clay and loam geotechnical properties are participated in one-dimensional statistical analysis. The distribution curves of measured parameters are plotted. The most suitable theoretical distribution curves are applied to the empirical ones based on the corresponding distribution law (normal named Gaussian or lognormal).

The one-dimensional statistical analysis for values of geotechnical properties of soils, which samples were selected across near karst cavities or crushed zones are executed separately.

Both, the lack of data on the size of karst cavities and crushed zones with the absence of precise methodic for calculating their horizontal size from vertical ones, make it difficult to determine the distance within which the overlying soils properties will be affected by the karst cavities or crushed zones. However, Shcherbakov and Kataev (2013) studying the large volume of factual material found the relation between vertical and horizontal morphometric parameters of surface karst form. Using this relation and the maximum vertical thickness of the karst cavities and crushed zones in the study area, we can determine the approximate horizontal value of their influence, in the particular case of 50–60 m.

The distribution curves of soil properties on the whole territory and separately subject to the karst cavities and crushed zones' presence were plotted after the one-dimensional statistical analysis. The curves reflect the distribution of the geotechnical properties. The peaks of the differential curves correspond to the most common values of the geotechnical properties. The range of the most common values is determined based on the mean value $M$ and the standard deviation $\sigma$ from the mean value and is equal to $M_i \pm \sigma$.

Using the integral distribution curves of the geotechnical properties on the whole territory and on the sites close to the the karst cavities and crushed zones, we can find a certain coefficient $k$ (1) which would represent the difference of the investigated parameters values (Fig. 12):

$$k = \frac{X^A_{P_{0,1}}}{X^B_{P_{0,1}}} \tag{3}$$

where $X^A_{P_{0,1}}$ is the investigated parameter value near the karst cavities and crushed zones with probability of 0.1, $X^B_{P_{0,1}}$ is the investigated parameter value on the whole territory with probability of 0.1.

Considering the values of investigated parameters for several probabilities (e.g. 0.1, 0.4, 0.7), we can find the average value of $k$, which can then be applied for similar areas. So it is possible to find areas of potential occurrence of the karst cavities and crushed zones using the distribution curves plotted on the basis of laboratory measurements of the overlying soil samples.

Further integral index is obtained based on complex assessment of the laboratory sample measurements—soil density $\rho$, soil void ratio $e$, cohesion $c$, and friction angle

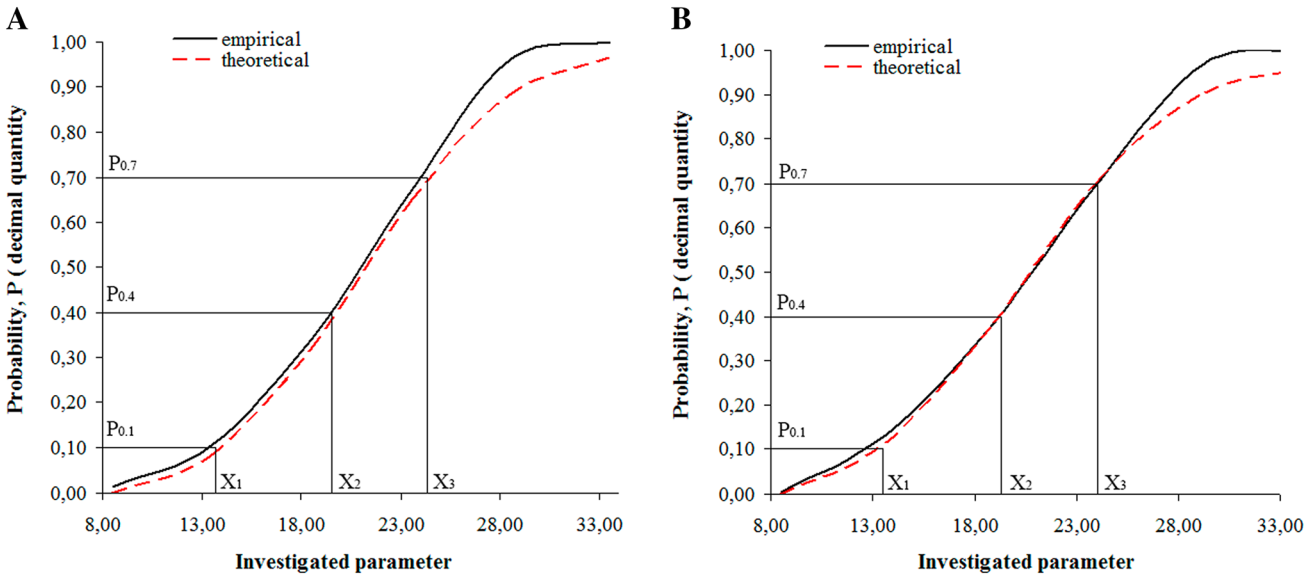


**Fig. 12** Integral distribution curves: **a**—near the karst cavities and crushed zones, **b**—on the whole territory

$\varphi$. These parameters are necessarily obtained during the civil engineering and karstological surveys of the overlying sediments. Besides they are used in current models of karst hazard assessments (Anikeev 2017; Kutepov 1986; Khomenko 2015). Thus, input data for the analysis can be involved from the engineering surveys without any additional investigations. Natural humidity, which is also a necessary characteristic obtained in civil engineering, is not considered in this research because of the constant variability and exposure to the anthropogenic impact.

The local analysis using statistical methods and computer modeling is carried out. The ordered sample is constructed and descriptive statistics is obtained for each factor. The average factor value in the study area ($M$) and the standard deviation ($\sigma$) are estimated. Further, the empirical and theoretical distribution curves were plotted in accordance with the random values distribution law determined earlier. The theoretical distribution curves indicate the intervals of background ($M \pm \sigma$) and anomalous ($C_a$) values:

$C_a \geq M \pm \sigma$—for friction angle and soil void ratio, $C_a \leq M \pm \sigma$—for soil density and specific cohesion.

The values of geotechnical properties are mapped using the sampling locations and ranged by the intervals on the distribution curves according to karst susceptibility which maximum (3 balls) matches with anomalous parameter values, minimum (1 ball) matches with background values. These maps are overlapped with each other to detect the weakened bedrock. The result of the overlapping is an integrated cartographic model which has zones of the maximum total score values corresponding to the areas with the highest probability of karst cavities and crushed zones appearance.

Testing of the research is carried out through a spatial analysis of the karst cavities and crushed zones location recorded in boreholes. The results are presented in a table in which the number of subterranean karst forms is spatially related to the categories of the integral model.

## Research results

The distribution curves of the overlying soil mechanical properties are plotted as the result of one-dimensional statistical analysis. The distribution of the friction angle and cohesion values is characterized by Gaussian law. The friction angle average value increases near the subterranean karst forms to 21.0 degrees (15.1–26.9°) from 20.3° (14.2–26.4°), as is typical on the whole territory. The variability of cohesion is the reverse: higher values are observed on the whole territory (9.5–30.5 kPa, average 20.0 kPa), and lower ones are typical in area near the subterranean karst forms (7.7–29.3 kPa, average 18.5 kPa). Using the integral curves (Drobinina et al. 2018) with consideration to the nature of the variability of properties, it is possible to find the average value of transition coefficients ($k$) from the background properties' values to anomalous ones. The nature of the variability of properties is characterized by course of changes in property values above cavities and crushed zones relative to property values on the whole territory. For the friction angle φ and the cohesion $c$, these coefficients are as follows:

(1) $k_{\varphi 0.1} = 1.07$, $k_{\varphi 0.4} = 1.05$, $k_{\varphi 0.1} = 1.03$, $k_{\varphi\ \text{average}} = 1.05$,
(2) $k_{c0.1} = 1.03$; $k_{c0,4} = 1.02$; $k_{c0.1} = 1{,}03$; $k_{c\ \text{average}} = 1.03$.

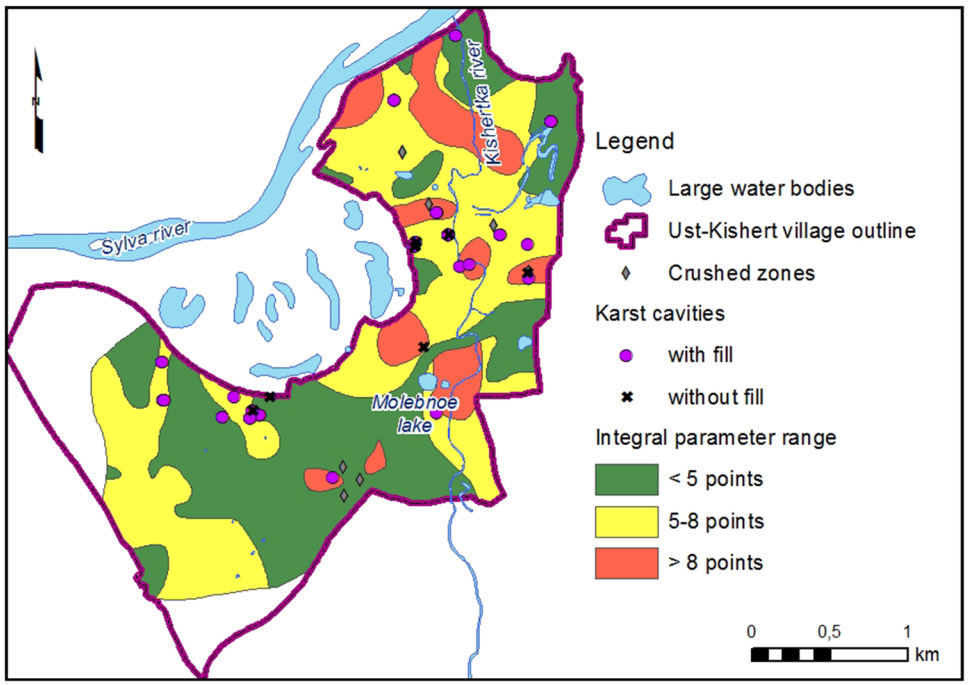


**Fig. 13** The zonation map of the karst susceptibility integral index (map projection: EPSG:28,410 Pulkovo 1942/ Gauss-Kruger zone 10; Drobinina 2016)

**Table 1** Quantitative assessment of karst-susceptible according to selected categories

| Karst susceptibility category | Integral parameter, points range | Area of the category ($km^2$) | Num. of karst forms, pcs | | Density of karst forms ($pcs./km^2$) | |
|---|---|---|---|---|---|---|
| | | | Crushed zones | Cavities | Crushed zones | Cavities |
| 1 | < 5 | 2.30 | 4 | 10 | 1.7 | 4.4 |
| 2 | 5–8 | 2.40 | 14 | 34 | 5.8 | 14.1 |
| 3 | > 8 | 0.70 | 6 | 16 | 8.5 | 22.7 |

The analysis of the overlying soil geotechnical properties is resulted in the integral model of karst susceptibility in the research area. The model is zoned into three categories with different integral indexes (parameters) (Fig. 13). The increase in the integral index is attended by the increase of possibility of karst cavity and crushed zones presence.

The territory with the average integral index has the greatest number of crushed zones and karst cavities. However, the highest density of subterranean karst forms ($pcs./km^2$) is confined to the areas with the maximum integral index (Table 1).

The karst susceptibility assessment of the Ust-Kishert village territory has been carried out earlier by Kovaleva (2015). The author analyzed the influence of geological and hydrogeological parameters of karst massif to the surface and subterranean karst forms distribution. The map of karst susceptibility has been created and the most and the least karst-susceptible intervals of the geological and hydrogeological parameters have been identified according to the data from 100 boreholes and the surface and subterranean karst forms distribution.

The spatial match of karst susceptibility categories is established when comparing these two models. Both models have the central part of the investigated territory as the most dangerous. The southern part, on the contrary, is characterized by a lesser danger.

## Conclusion

The karst cavity influence on the mechanical properties of the overlying soils could be revealed by the computer simulation of the soil stress condition. The one-dimensional statistical analysis of soil properties values on the whole territory and separately near subterranean karst forms confirms it.

The distribution of the friction angle and cohesion values is characterized by Gaussian law. The friction angle average value increases near the subterranean karst forms, but the variability of cohesion is the reverse; higher values are observed on the whole territory. Using the integral curves (Drobinina et al. 2018) with consideration to the nature of the variability of properties, it is possible to find the

average value of transition coefficients from the background properties values to anomalous ones. The transition coefficients could be used for potential cavities and crushed zones localization where bedrock is not reveal by boreholes.

The proposed integral model of karst susceptibility is based on the evaluation of integral index based on complex assessment of the overlying soil geotechnical properties. The values of geotechnical properties are mapped using the sampling locations and ranged by the intervals on the distribution curves according to karst susceptibility which maximum (3 balls) matches with anomalous parameter values, minimum (1 ball) matches with background values.

The zonation map of the karst susceptibility integral index demonstrates areas different in possibility of the subterranean karst form occurrence and consequently different in sinkholes formation probabilities. The increase in the integral index is attended by the increase of possibility of karst cavity and crushed zones presence. The karst cavities and crushed zones exact locations are not determined by the model. However, the direction of further detailed study could be outline through this analysis.

## References


Anikeev AV (2017) Sinkholes and subsidence of the earth's surface in karst areas: mechanisms of formation, forecast and risk assessment. RUDN, Moscow **(in Russian)**

Brinkmann R, Wilson K, Elko N, Seale LD, Florea L, Vacher HL (2007) Sinkhole distribution based on pre-development mapping in urbanized Pinellas County, Florida, USA. From: Parise, M. & Gunn, J. (eds) Natural and Anthropogenic Hazards in Karst Areas: Recognition, Analysis and Mitigation. Geological Society, London, Special Publications, 279:5–11. Doi: 10.1144/SP279.2

Churinova MV (ed) (1968) Reference book on engineering geology. Nedra, Moscow **(in Russian)**

Dreybrodt W (2006) Dissolution: evaporite rocks. In: Gunn J (ed) Encyclopedia of caves and karst science. Fitzroy Dearborn, New York, pp 617–621

Drobinina E, Kovaleva T, Koriakina A (2018) Investigation of the local variation of physical and mechanical properties of the covering deposits in order to hazard assessment of karst (on the example of sulfate-carbonate karst of Permsky kray, Russia). In: Symposium KARST 2018—expect the unexpected. Trebinje, pp 135–142

Drobinina EV (2016) Investigation of local changes of physical and mechanical properties of overlying soils as indicators of the disintegration of rocks zone in the karst massif. In: Problems of geology and subsoil development, Tomsk, pp 548–550 (**in Russian**)

Ford DC, Williams P (2007) Karst hydrogeology and geomorphology. Wiley, Chichester

Gorbunova KA, Andreychuk VN, Kostarev VP (1992) Maksimovich NG. Karst and caves of the Perm region, Perm **(in Russian)**

Gutiérrez F, Cooper AH (2013) Surface morphology of gypsum karst. In: Frumkin A (ed) Treatise on geomorphology, vol 6. Elsevier, Amsterdam, pp 425–437

Gutiérrez F, Parise M, De Waele J, Jourde H (2014) A review on natural and human-induced geohazards and impacts in karst. Earth Sci Rev 138:61–88. https://doi.org/10.1016/j.earscirev.2014.08.002

Kataev VN (2004) Fundamentals of structural karstology. PSU, Perm **(in Russian)**

Kataev VN (1994) System approach in the stability of karst massifs analysis. Bull Perm Univ Geol Issue 3:127–144 **(in Russian)**

Kaufmann G (2014) Geophysical mapping of solution and collapse sinkholes. J Appl Geophys 111:271–278

Khomenko VP (2015) Karst sinkhole formation: mechanism and hazard assessment. In: Environmental safety and construction in karst areas. Proceedings of the international symposium. Russia, Perm, pp 50–60 (**in Russian**)

Kovaleva TG (2015) The results of the karst hazard assessment of the carbonate-sulfate karst areas on the basis of geological and hydrogeological factors. In: Environmental safety and construction in karst areas. Proceedings of the international symposium. Russia, Perm, pp 173–176 (**in Russian**)

Kutepov VM (1986) The stability of karst areas assessment by the method of stress analysis of rock massifs Overview and recommendations. TSP NTGO, Moscow **(in Russian)**

Margiotta S, Negri S, Parise M, Quarta TAM (2016) Karst geosites at risk of collapse: the sinkholes at Nociglia (Apulia, SE Italy). Environ Earth Sci 75(1):1–10. https://doi.org/10.1007/s12665-015-4848-y

Milanović P (2018) Karst Hydrogeology. Belgrade

Nisio S, Caramanna G, Ciotoli G (2007) From: PARISE, M. & GUNN, J. (eds) Natural and anthropogenic hazards in karst areas: recognition, analysis and mitigation. Geological Society, London, Special Publications, 279, 23–45. DOI: 10.1144/SP279.4

Paniukov PN (1962) Engineering geology. Gosgortekhizdat, Moscow **(in Russian)**

Parise M (2015) A procedure for evaluating the susceptibility to natural and anthropogenic sinkholes. Georisk 9(4):272–285

Parise M, Closson D, Gutiérrez F, Stevanović Z (2015) Anticipating and managing engineering problems in the complex karst environment. Environ Earth Sci 74:7823–7835. https://doi.org/10.1007/s12665-015-4647-5

Postoev GP (2013) The limit state and deformation of soils in the massif (landslides, sinkholes, ground base subsidence. Sankt-Peterburg, Moscow **(in Russian)**

Shcherbakov SV, Kataev VN (2013) Towards assessment of morphometric characteristics of karst forms. In: Engineering geology, vol 1. PNIIIS, Moskow, pp 56–64 (**in Russian**)

Shilova AV, Kovaleva TG (2015) Influence of overlying mass on the development of karst forms on the example of the Ust-Kishert village, the Perm region. In: Environmental safety and construction in karst areas. Perm, pp 351–355 (**in Russian**)

Terzaghi K (1996) Soil mechanics in engineering practice, 3rd edn. New York

Varnes DJ (1984) Landslide hazard zonation: a review of principles and suggested practice. UNESCO, Paris

Waltham T, Lu Z (2007) Natural and anthropogenic rock collapse over open caves. In: Parise M, Gunn J (eds) Natural and anthropogenic hazards in karst areas: recognition, analysis and mitigation, vol 279. Geological Society Special Publications, London, pp 13–21. https://doi.org/10.1144/SP279.3

Waltham T, Bell F, Culshaw M (2005) Sinkholes and subsidence: karst and cavernous rocks in engineering and construction. Springer, Berlin

Zhou W, Beck BF (2011) Engineering issues on karst. In: van Beynen P (ed) Karst management. Springer, Dordrecht, pp 9–45. https://doi.org/10.1007/978-94-007-1207-2_2